

CT-based radiomic signature predicts distant metastasis in lung adenocarcinoma

Citation for published version (APA):

Coroller, T. P., Grossmann, P., Hou, Y., Velazquez, E. R., Leijenaar, R. T. H., Hermann, G., Lambin, P., Haibe-Kains, B., Mak, R. H., & Aerts, H. J. W. L. (2015). CT-based radiomic signature predicts distant metastasis in lung adenocarcinoma. *Radiotherapy and Oncology*, 114(3), 345-350. <https://doi.org/10.1016/j.radonc.2015.02.015>

Document status and date:

Published: 01/03/2015

DOI:

[10.1016/j.radonc.2015.02.015](https://doi.org/10.1016/j.radonc.2015.02.015)

Document Version:

Publisher's PDF, also known as Version of record

Document license:

Taverne

Please check the document version of this publication:

- A submitted manuscript is the version of the article upon submission and before peer-review. There can be important differences between the submitted version and the official published version of record. People interested in the research are advised to contact the author for the final version of the publication, or visit the DOI to the publisher's website.
- The final author version and the galley proof are versions of the publication after peer review.
- The final published version features the final layout of the paper including the volume, issue and page numbers.

[Link to publication](#)

General rights

Copyright and moral rights for the publications made accessible in the public portal are retained by the authors and/or other copyright owners and it is a condition of accessing publications that users recognise and abide by the legal requirements associated with these rights.

- Users may download and print one copy of any publication from the public portal for the purpose of private study or research.
- You may not further distribute the material or use it for any profit-making activity or commercial gain
- You may freely distribute the URL identifying the publication in the public portal.

If the publication is distributed under the terms of Article 25fa of the Dutch Copyright Act, indicated by the "Taverne" license above, please follow below link for the End User Agreement:

www.umlib.nl/taverne-license

Take down policy

If you believe that this document breaches copyright please contact us at:

repository@maastrichtuniversity.nl

providing details and we will investigate your claim.



CT based radiomic signature

CT-based radiomic signature predicts distant metastasis in lung adenocarcinoma



Thibaud P. Coroller^{a,c,1,*}, Patrick Grossmann^{a,c,1}, Ying Hou^a, Emmanuel Rios Velazquez^a, Ralph T.H. Leijenaar^c, Gretchen Hermann^a, Philippe Lambin^c, Benjamin Haibe-Kains^{d,e}, Raymond H. Mak^{a,1}, Hugo J.W.L. Aerts^{a,b,c,1,*}

^a Department of Radiation Oncology; ^b Department of Radiology, Dana-Farber Cancer Institute, Brigham and Women's Hospital, Harvard Medical School, Boston, USA; ^c Department of Radiation Oncology (MAASTRO), GROW Research Institute, Maastricht University, The Netherlands; ^d Princess Margaret Cancer Centre, University Health Network, Toronto; and ^e Medical Biophysics Department, University of Toronto, Canada

ARTICLE INFO

Article history:

Received 29 October 2014
Received in revised form 6 February 2015
Accepted 15 February 2015
Available online 4 March 2015

Keywords:

Radiomics
Lung adenocarcinoma
NSCLC
Quantitative imaging
Biomarkers
Distant metastasis

ABSTRACT

Background and purpose: Radiomics provides opportunities to quantify the tumor phenotype non-invasively by applying a large number of quantitative imaging features. This study evaluates computed-tomography (CT) radiomic features for their capability to predict distant metastasis (DM) for lung adenocarcinoma patients.

Material and methods: We included two datasets: 98 patients for discovery and 84 for validation. The phenotype of the primary tumor was quantified on pre-treatment CT-scans using 635 radiomic features. Univariate and multivariate analysis was performed to evaluate radiomics performance using the concordance index (CI).

Results: Thirty-five radiomic features were found to be prognostic (CI > 0.60, FDR < 5%) for DM and twelve for survival. It is noteworthy that tumor volume was only moderately prognostic for DM (CI = 0.55, p -value = 2.77×10^{-5}) in the discovery cohort. A radiomic-signature had strong power for predicting DM in the independent validation dataset (CI = 0.61, p -value = 1.79×10^{-17}). Adding this radiomic-signature to a clinical model resulted in a significant improvement of predicting DM in the validation dataset (p -value = 1.56×10^{-11}).

Conclusions: Although only basic metrics are routinely quantified, this study shows that radiomic features capturing detailed information of the tumor phenotype can be used as a prognostic biomarker for clinically-relevant factors such as DM. Moreover, the radiomic-signature provided additional information to clinical data.

© 2015 Elsevier Ireland Ltd. All rights reserved. Radiotherapy and Oncology 114 (2015) 345–350

Lung cancer is the most deadly cancer worldwide for both men and women [1]. Non-small cell lung cancer (NSCLC) is the most common type of lung cancer (85–90% of all lung cancers) and adenocarcinoma is the most common subtype (about 40% of all lung cancers) of NSCLC. Patients with locally advanced (stage II–III) lung adenocarcinomas are typically treated with combined modality therapy including chemotherapy with local therapy including radiation therapy and/or surgery, but overall survival remains low due to a high risk of local recurrence and distant metastasis (DM) after treatment. Despite the use of concurrent chemotherapy

with local therapy, the incidence of DM after combined modality therapy is as high as 30–40% in prospective trials [2–4]. However, large randomized trials studying consolidation chemotherapy after concurrent chemotherapy and radiation therapy have not shown improvement in overall survival with additional chemotherapy [5,6] likely because there was no selection of patients at the highest risk of DM. Therefore, developing better biomarkers to predict patients at the highest risk of DM may help identify sub-groups who benefit from intensification of systemic therapy and is crucial for improving outcomes.

Due to recent technological advances in medical imaging it is possible to capture tumor phenotypic characteristics non-invasively. The most widely used imaging modality is Computed-Tomography (CT), which can quantify tissue density. In lung cancer, CT imaging is routinely used for patient management, including diagnosis, radiation treatment planning and surveillance.

* Corresponding authors at: Dana-Farber Cancer Institute, Brigham and Women's Hospital, Harvard Medical School, 450 Brookline Ave, JF518, Boston, MA 02115-5450, USA.

E-mail addresses: tcroller@roc.harvard.edu (T.P. Coroller), Hugo_Aerts@dfci.harvard.edu (H.J.W.L. Aerts).

¹ Equal contribution.

Tumor phenotypic differences (e.g., shapes irregularity, infiltration, heterogeneity or necrosis) can be quantified in CT images using radiomic features. Radiomics [7–9] aims to provide a comprehensive quantification of the tumor phenotype by analyzing robustly [10–12] a large set of quantitative data characterization algorithms. Biomarkers based on quantitative features have demonstrated strong prognostic performance across a range of cancer types and investigators have reported that these features are associated with clinical outcomes and underlying genomic patterns [13–26]. Radiomics has significant clinical potential, as it can be applied to routinely acquired medical imaging data at low costs.

In this manuscript we present a radiomic analysis to identify biomarkers of DM in patients treated with chemoradiation (chemoRT) for locally advanced lung adenocarcinoma. In a discovery dataset, we extracted 635 radiomics features to identify the optimal features for predicting metastasis. Only a limited number of features with high performance for predicting DM were tested in the independent validation dataset. We evaluated the ability of radiomic features to predict DM or overall survival, and how these features compare with basic metrics (e.g., volume, diameter) as prognostic factors [27–30].

Materials and methods

Patient characteristics

This study is an Institutional Review Board-approved analysis of CT for treatment simulation from North-American NSCLC patients receiving chemoRT at our institution from 2001 to 2013. We limited the patient population to pathologically-confirmed lung adenocarcinoma with locally advanced disease (overall stage II–III) [30]. Patients with surgery or chemotherapy before the scheduled radiation therapy planning CT date were excluded from the study. Patients treated before July 2009 were included in the discovery Dataset1 ($n = 98$), and after July 2009 in an independent validation Dataset2 ($n = 84$). In total 182 patients were included in our analysis.

Clinical endpoints

Patients were followed up every three to 6 months after treatment, and surveillance chest CT scans with contrast (unless patient's contraindication, e.g., allergy or renal dysfunction) were

performed to assess treatment response or tumor progression based on US national guidelines (NCCN). The primary endpoint of this study was distant metastasis (DM), which was defined as progression of disease to other organs as assessed in surveillance scans, and time to DM was defined as time from start of radiation to date of DM or censoring (date of last scan). Overall survival was analyzed as a secondary endpoint, and was defined as the time between the start of radiation treatment and last day of follow up or date of death.

Clinical variables

The conventional clinical prognostic factors (CPFs) used for this study included tumor grade (1-Well differentiated, 2-Moderately differentiated, 3-Poorly differentiated and 4-Not available), Eastern Cooperative Oncology Group (ECOG) performance status (PS) [31], TNM stage per the American Joint Committee on Cancer (AJCC) staging system (7th edition) [30]; CT-based measurements commonly utilized in the clinic (e.g., tumor volume and maximal tumor diameter measured on single axial slice), and treatment characteristics. Sub-group analyses of clinical variables were performed (e.g., overall stage II vs. IIIA vs. IIIB) and can be found in Table S1 (Supplement II.1).

CT acquisition and segmentation

Planning CT was performed according to standard clinical scanning protocols at our institution with a GE “LightSpeed” CT scanner (GE Medical System, Milwaukee, WI, USA). The most common pixel spacing was (0.93 mm, 0.93 mm, 2.5 mm) for CT. The primary lung tumor was delineated manually on Eclipse (Varian Medical System, Palo Alto, CA, USA). It was first contoured in the abdomen window to identify the boundaries with the chest wall or other soft tissues, then in the lung window to capture the maximum extent in the lung parenchyma. All contours were reviewed by an experienced radiation oncologist (R.H.M.).

Radiomic feature extraction

Radiomic features have the capacity to capture tumor phenotype differences by examining a large set of quantitative features (Fig. 1). The feature extraction was performed in MATLAB 2013b

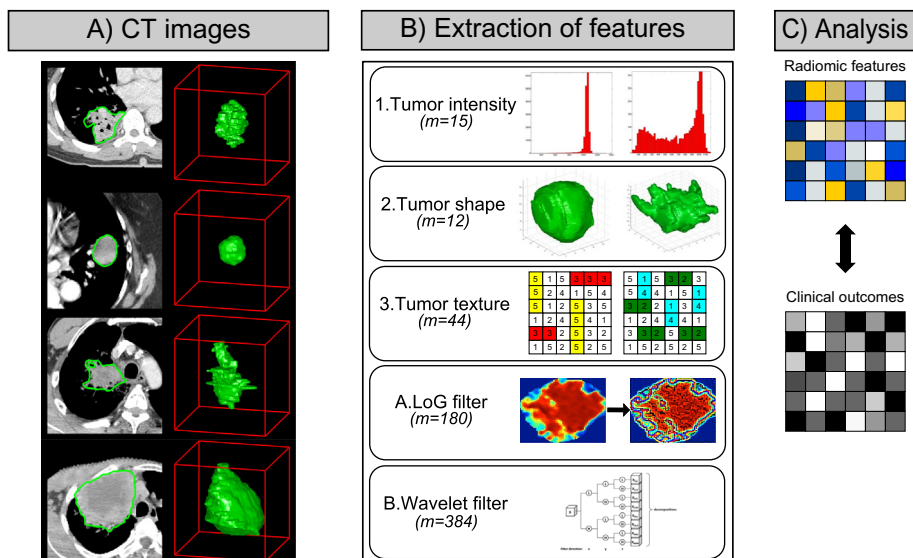


Fig. 1. (A) Differences between lung primary tumors with a same histology are apparent on CT images (3D model on the right and CT contours on the left). CT images of primary tumors contain critical information that can be used to predict outcomes or assess the RT treatment response. (B) To quantify this information, a large set of features ($m = 635$) is used to capture the tumor phenotype. It includes 1) intensity, 2) shape and 3) texture based features. Also, A) Laplacian of Gaussian (LoG) and B) Wavelet filtered features were investigated. (C) The final step is to link radiomic information to clinical data.

(Mathworks, Natick, MA, USA) using an in-house developed toolbox running on the Computational Environment for Radiotherapy Research (CERR) [32]. DICOMs files (CT images + tumor contours) were imported into CERR to extract the radiomic features. The radiomic feature set included is described in detail in the Supplement I.

Feature selection

Feature selection for the radiomic signature was performed with the minimum redundancy maximum relevance (mRMR) algorithm implemented in the mRMRe [33] package version 2.0.4 in R. The mRMR algorithm is an entropy based feature selection method, which starts by calculating the mutual information (MI) between a set of features and an outcome variable. MRMR ranks the input features by maximizing the MI with respect to outcome and minimizing the average MI of higher ranked features. Here, survival objects as implemented in R with “Survcomp” package [34] were used as outcome to select complementary features with respect to DM or survival.

Among available clinical covariates, those with $p < 0.1$ on univariate analysis of DM using a Log-Rank test were included into a multivariate clinical prognostic model.

Data analysis

Univariate and multivariate analyses were performed for this study. All analysis were performed on Dataset1, leaving Dataset2 as an independent validation cohort for evaluating the radiomic signature.

Statistical analysis was conducted using the survcomp [34] package version 1.12 and rmeta [35] package version 2.16 in Bioconductor [36]. Prognostic performances were evaluated by the concordance index [37] (CI), which is the probability that among two randomly drawn samples, the sample with the higher risk value has also the higher chance of experiencing an event (e.g., death or development of DM). CIs were either directly computed for continuous variables or on the predictions of a univariate Cox model with clinical categorical variables. Kaplan–Meier and Log-Rank statistics were used to analyze the univariate discrimination of survival and DM groups by imaging features and clinical covariates. To build the multivariate radiomic signature for DM, Cox regression models were trained on Dataset1 for selected prognostic variables and the predictions by these models were validated on Dataset2. Features were incrementally added to the model according to the relevance rank calculated by mRMR [33]. Intermediate models were

tested by repeated random sub-sampling cross validation with 1,000 iterations on Dataset1. Once the mean CI of the growing model dropped, the corresponding feature set was retained selected as the final model. Only this selected model was and validated on Dataset2. Significance of CIs was assessed by bootstrapping subsamples of size 100 with 100 repetitions for (A) true survival data and (B) random permutations of survival data, and comparing the empirical distributions of (A) and (B) by a one-sided Wilcoxon signed rank test. The same procedure was used to assess if a CI was higher than another CI. To correct for multiple comparisons, we additionally adjusted P -values by the false-discovery-rate (FDR) procedure according to Benjamini and Hochberg [38]. All statistical analysis was performed using the R software [39] version 3.0.2.

Results

The majority of all patients were female (62.6%) and the median age at start of treatment was 64 years (range: 35–93 years). The median follow-up time was 23.7 months (range: 1.8–119.2 months) and the median survival time was 24.7 months (range: 1.8–119.2 months). The median time to distant metastasis (DM) was 13.4 months (range: 0.3–117.5 months). Patient characteristics, clinical outcomes are shown in Table 1.

Time to DM was similar between Dataset1 and Dataset2 (p -value < 0.36), as for the numbers of DM (p -value < 0.45). However, survival (p -value < 0.005) and follow-up times (p -value < 0.007) were significantly different in Dataset1.

We investigated the association of radiomics data with DM and overall survival. In Fig. 2 the association of the imaging features with DM and survival in the discovery Dataset1 is shown. Of the complete radiomic feature set ($m = 635$), a total of 520 (81.88%) and 582 (91.65%) features were significant from random (FDR $< 5\%$) for DM and survival, respectively. A total of 445 radiomic features were significant for both DM and survival. A high linear relationship was observed ($R^2 = 0.92$, p -value $< 2.7 \times 10^{-243}$), for the features significant for both DM and survival. It is noteworthy that LoG features had the highest performance compared to the other feature groups.

Among all features, thirty-five radiomics features were strongly prognostic (CI > 0.60 and FDR $< 5\%$) for DM (Table S2 in the Supplement II.3). Twelve features were found prognostic for survival. Specific details on statistic values of these features can be found in Table S3 in Supplement II.3. Between these two top performing feature sets there were four common prognostic features for both DM and survival. All of them were LoG based features (3 entropy and 1 standard deviation).

Table 1

Patient characteristics and outcomes are reported for each datasets. For categorical variables, actual numbers are reported for each category (format A/B/C). Statistical comparison between dataset 1 and 2 was computed using Chi Square (categorical variables) or Wilcoxon rank sum test (continuous variables).

	Overall dataset ($n = 182$) Median (range)	Dataset 1 ($n = 98$) Median (range)	Dataset 2 ($n = 84$) Median (range)	P -value
Age [years]	64 (35–93)	62 (41–86)	65 (35–93)	0.63
Gender [F/M]	114(62.6%)/68(37.4%)	66(67.3%)/32(32.7%)	48(57.1%)/36(42.9%)	0.29
Overall stage [IIA/IIIB/IIIA/IIIB]	6/3/101/72	2/1/55/40	4/2/46/32	0.65
T-stage [T1a/T1b/T2a/T2b/T3/T4]	19/23/50/19/39/32	14/10/30/10/17/17	5/13/20/9/22/15	0.26
N-stage [N0/N1/N2/N3]	13/17/97/55	5/9/53/31	8/8/44/24	0.70
Performance status [0/1/2/3]	81/91/8/2	36/57/5/0	45/34/3/2	0.04
Tumor grade [1/2/3/X]	4/28/92/58	3/11/47/37	1/17/45/21	0.12
Follow-up [months]	23.7 (1.8–119.2)	28.9 (1.8–119.2)	19.5 (3.1–54.9)	0.007
Survival [months]	24.7 (1.8–119.2)	29.7 (1.8–119.2)	21.4 (3.4–54.9)	0.005
Time to distant metastasis [months]	13.4 (0.3–117.5)	13.6 (0.3–117.5)	13.3 (0.7–49.6)	0.36
Distant metastasis [No/Yes]	69(37.9%)/113(62.1%)	34(34.7%)/64(65.3%)	35(41.7%)/49(58.3%)	0.45
Radiation dose delivered $\leq 54 / \leq 60 / \leq 66 / \leq 66$ [Gray]	60(32.97%)/ 30(16.48%)/ 70(38.45%)/ 22(12.1%)	28(28.57%)/ 17(17.35%)/ 33(33.67%)/ 20(20.41%)	32(38.10%)/ 13(15.48%)/ 37(44.04%)/ 2(2.38%)	0.002
Chemotherapy sequence [concurrent/adjuvant/induction]	175/79/28	95/38/22	80/41/6	0.024

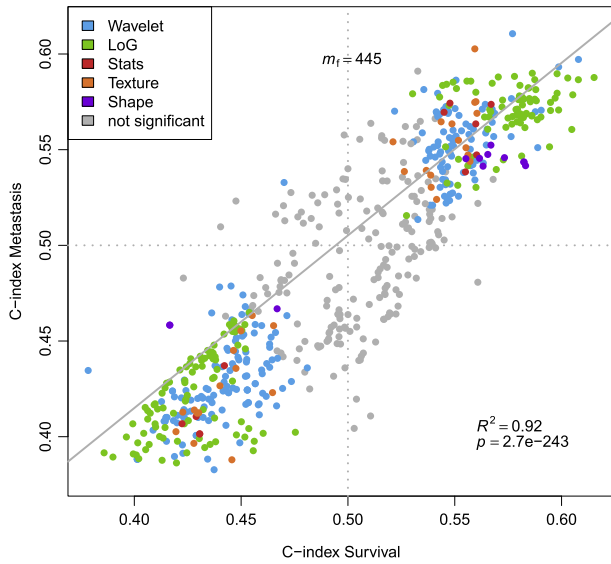


Fig. 2. Univariate performances of prognostic features for Distant Metastasis (DM) and survival. Each point refers to the CI of a feature evaluating the power of feature to predict metastasis, respectively, survival. Colors refer to the type of feature. Features whose CI estimation was not significant (FDR < 5%) for both DM and survival are shown in gray. Overall, 445 of these pairs of CIs are considered to be significant estimates. Linear regression for all significant pairs of CIs yielded an R-squared value of 0.92 (*F*-test, *p*-value < 2.7×10^{-243}).

We compared the top 15 features that had the highest CIs (Top15), with tumor volume and diameter (equivalent to basic metrics). The Top15 radiomic features had notably higher CIs compared to tumor volume and diameter (Fig. 3A).

We also investigated the association of CPFs with DM in our data set. Three clinical parameters appeared to be significant univariate prognostic factors: Overall Stage (CI = 0.63, *p*-value < 6.78×10^{-14}), Gender (CI = 0.63, *p*-value < 2.35×10^{-11}) and tumor grade (CI = 0.61, *p*-value < 2.35×10^{-11}). Clinical parameters, ranked by their CI are displayed in Fig. 3B. Overall stage and gender yielded a higher CI than the radiomic features, although their 95% confidence interval is wider compared to the radiomic features.

An mRMR based feature selection on all features on Dataset1 (*n* = 98) was performed to reduce redundancy and select a

potential set of complementary and prognostic features. From this new ranking, the 15 highest mRMR-ranked features were kept after feature selection to build the radiomic signature. A multivariate Cox regression model to predict DM was developed. Features were iteratively added in order of high to low mRMR rank on Dataset1, and Dataset2 was used for independent validation. The combination that yielded the maximum CI on the discovery Dataset1 before dropping was defined as the optimal radiomic signature for predicting DM. This signature consists of three features: (1) Wavelet HHL-Skewness, (2) Gray-Level Co-occurrence Matrix-Cluster shade, and (3) LoG 5 mm 2D-Skewness. Cluster shade is a textural feature sensitive to tumor heterogeneities. Skewness is a first-order feature that measures the asymmetry of the histogram from the mean, which here is associated with two different filters LoG and Wavelet.

As a final step, we compared the radiomic signature to a clinical Cox regression model containing covariates that significantly discriminated between patients with and without DM in Dataset1 in univariate analysis. The final model contained overall stage and tumor grade. This clinical model showed moderate prognostic power when applied to Dataset2 with coefficients trained on Dataset1 (CI = 0.57, *p*-value < 1.03×10^{-7}). Combining the clinical and radiomic signature (trained on Dataset1) showed a significantly (*p*-value < 1.56×10^{-11}) higher association with DM when applied to Dataset2 (CI = 0.60, *p*-value < 3.57×10^{-16}), compared to the clinical model. A median split of the patient prediction scores from applying the combined model on Dataset2 yielded a significant difference (*p*-value = 0.049) for metastasis-free probability estimates (Fig. 4).

Discussion

Medical imaging gives valuable information for diagnostic, treatment planning or surveillance of cancer patients. Routinely, basic metrics are extracted from these images to utilize as a prognostic factor [27–30], or to assess treatment response. However, there is much more tumor phenotypic information captured in these images. Radiomics are able to quantify tumor phenotypical differences from medical images by using a large set of imaging features that can be linked to clinical factors of the tumors. In this study we extracted 635 radiomic features from a total of 182 lung cancer patients treated with chemoRT to assess the ability of radiomic

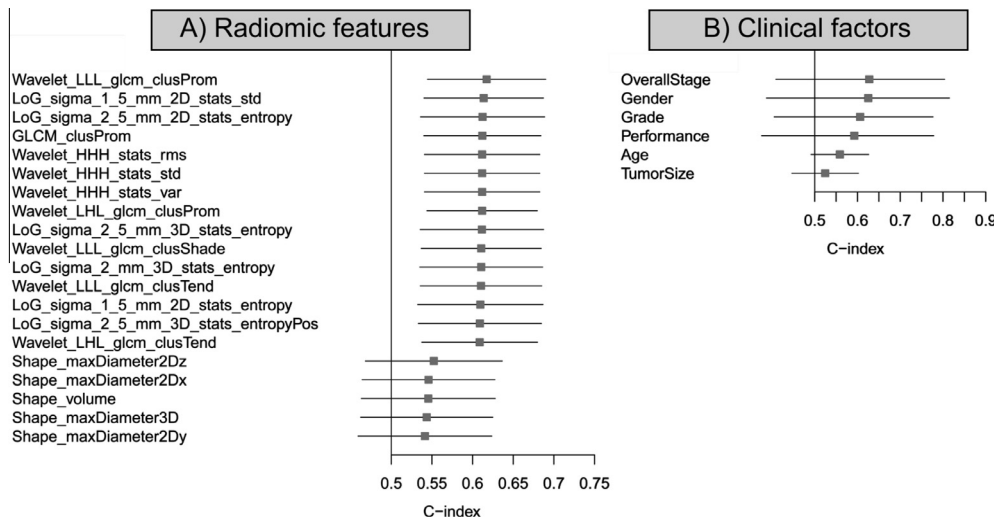


Fig. 3. (A) Forest plot of the 15 best performing radiomic features for Distant Metastasis on univariate analysis (Dataset1, *n* = 98). Radiomics equivalent of basic metrics (diameter and volume) was added for comparison. (B) Forest plot of the clinical factors. The absolute C-indices and their 95% confidence interval are shown.

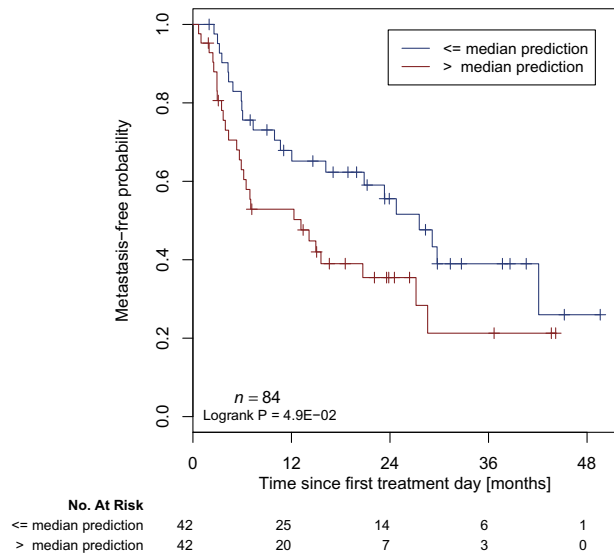


Fig. 4. Kaplan Meier curves according to the combined model predicting score to predict metastasis-free probability in an independent dataset. A significant survival difference appears between patients with a high or low risk of Distant Metastasis (Dataset2, $n = 84$, Log-Rank test, p -value < 0.049).

features as a prognostic biomarker for distant metastasis (DM), and we validated a radiomic-based signature on an independent validation dataset. Since DM remains a major cause of mortality in 30–40% of patients with locally advanced lung adenocarcinoma, early identification of patients at the highest risk of developing DM would allow clinicians to adapt treatment such as incorporating consolidation chemotherapy to improve outcomes. Moreover, the theoretical benefit of consolidation chemotherapy has not been shown in large randomized studies to date. It is likely because there was no selection of patients at the highest risk of distant metastases (i.e. patients who were at low risk of distant metastases were included in these trials and would not need additional treatment). Future trial design to demonstrate benefits of consolidation chemotherapy will likely require stratification to identify those at the highest risk of distant metastases and may benefit most from additional treatment.

We observed strong individual correlations between clinical outcomes and quantitative imaging features. A large number of features were significant from random to predict DM (91%) and survival (82%) in univariate analysis after correction for multiple testing. Moreover, a high linear correlation was found among those 445 features that were significant factors of both DM and survival ($R^2 = 0.92$, p -value $< 2.7 \times 10^{-243}$). This high linear correlation is expected as there is a high correlation between DM and survival (DM greatly impact patient survival, See Table S4 in the Supplement II.4). Only a small number of features, 35 for DM and for 12 survival, were prognostic, as defined by a CI > 0.6 and FDR $< 5\%$.

Although we tested a large number of features, to minimize any risk of over-fitting or bias, we performed a robust validation approach: all analysis steps, mRMR feature selection, and model fitting were performed on Dataset1 ($n = 98$) and the results validated on an independent validation Dataset2 ($n = 84$). With this approach we found a multivariate radiomic DM signature consisting of three features that yielded a high prognostic performance for DM in Dataset1 (CI = 0.61). Combining the radiomic signature to clinical predictors showed significant improvement (p -value $< 1.56 \times 10^{-11}$), compared to the clinical predictors alone.

A recent study from Fried et al. [22] investigated DM prediction for NSCLC patients. They found a significant model DM (P -value = 0.005) using both texture features and CPFs. The model used consisted of eight parameters (two CPFs and six textures). In another study, Ganeshan et al. [15] applied textural analysis to find

univariate prognostic factors for survival. They focused on two imaging features (uniformity, associated with two LoG filter). In our analysis, these features were significant from random but lowly ranked by their CI value (184th and 146th CI-ranked features in Dataset1). However, major differences in study design and implementation made it difficult to compare them objectively. Fried et al. [22] used leave-one out cross validation to validate their model instead of an independent validation dataset. Ganeshan et al. [15] only used one CT image slice (presenting the largest cross section) to calculate their features when we used the whole primary tumor. Finally, both these studies have a smaller patient cohort, $n = 54$ [7] and $n = 91$ [22], and had mixed histology patients. Our analysis calculated the features from the complete 3D tumor volume, contained only a single histology of NSCLC (adenocarcinoma), and is based on larger cohorts ($n = 182$) with an independent validation dataset for the radiomic signature.

A complementary point of the study was to compare basic metrics [27–29] to radiomic features as prognostic factors for DM. The first observation made was that Shape-Maximum diameter (in every direction $x/y/z$) is a better univariate prognostic factor than the maximal tumor diameter on an axial slice reported by a radiologist. The advantage of the radiomic shape features is that they can be automatically acquired, reproducible [10–12], and take into account the whole tumor volume, whereas clinically assessed tumor diameters are manually drawn on a CT slice and are therefore limited to one dimension of the tumor. Furthermore, shape or size-based features were not in the top ranked features in our study. Total tumor volume, has been associated with survival in stage I–III NSCLC patients treated with radiation therapy in a study from Etiz et al. [28], and a prior study from our institution by Alexander et al. [29] also demonstrated an association between primary tumor volume and overall survival, but not risk of distant metastasis. In our study, volume was ranked only the 405th (CI = 0.55) and 224th (CI = 0.56) best univariate prognostic factor for DM and survival respectively in Dataset1. Thus, while basic metrics such as size and volume have historically been used as used in the clinical setting because such data are easily acquired, radiomic shape and size measurements can provide stronger prognostic factors.

A short-coming of our study is the variability in CT acquisition and reconstruction parameters. Our dataset includes patients from 2001 to 2013. During this time period, the standard of care for CT acquisition has evolved, differences appeared between our cohorts for some factors (Table 1). However, despite this variability in the imaging data (evolution of hardware, progress in informatics), radiomics was able to detect a strong signal to predict DM despite a temporal split. Additionally, clinical outcomes are provided by one center, which makes it hard to evaluate the generalizability of outcomes to other institutions. However, in comparison with a recent study [20] investigating clinical outcomes from another center, patient characteristics or outcomes were comparable. Future work would therefore involve studying the DM signature in other histologies and in independent validation sets from other institutions, assessing its generalizability to all NSCLC.

In conclusion, this study demonstrated strong association between radiomic features and DM for patients with locally advanced adenocarcinoma; and presented an independently validated radiomics signature for DM. This signature would allow early identification of patients with locally advanced lung adenocarcinoma at risk of developing DM, allowing clinicians to individualize treatment (such as intensification of chemotherapy) to reduce the risk of DM and improve survival.

Disclaimer

None.

Source of support

Authors acknowledge financial support from the National Institute of Health (NIH-USA U01CA190234). Authors acknowledge financial support from the QuIC-ConCePT project, which is partly funded by EFPI A companies and the Innovative Medicine Initiative Joint Undertaking (IMI JU) under Grant Agreement No. 115151. This research is also supported by the Dutch technology foundation STW (Grant No. 10696 DuCAT), which is the applied science division of NWO, and the Technology Programme of the Ministry of Economic Affairs. Authors also acknowledge financial support from EU 7th framework program (EURECA, ARTFORCE), NGI Pre-Seed Grant (No. 93612005), Kankeronderzoekfonds Limburg from the Health Foundation Limburg and the Dutch Cancer Society (KWF UM 2011-5020, KWF UM 2009-4454, KWF MAC 2013-6089).

Conflict of interest

None declared.

Appendix A. Supplementary data

Supplementary data associated with this article can be found, in the online version, at <http://dx.doi.org/10.1016/j.radonc.2015.02.015>.

References

- [1] Siegel R, Ma J, Zou Z, Jemal A. Cancer statistics, 2014: cancer Statistics, 2014. *CA Cancer J Clin* 2014;64:9–29.
- [2] Albain KS, Swann RS, Rusch VW, Turrisi AT, Shepherd FA, Smith C, et al. Radiotherapy plus chemotherapy with or without surgical resection for stage III non-small-cell lung cancer: a phase III randomised controlled trial. *Lancet* 2009;374:379–86.
- [3] Curran WJ, Paulus R, Langer CJ, Komaki R, Lee JS, Hauser S, et al. Sequential vs. concurrent chemoradiation for stage III non-small cell lung cancer: randomized phase III trial RTOG 9410. *J Natl Cancer Inst* 2011;103:1452–60.
- [4] Bradley JD, Paulus R, Komaki R, Masters GA, Forster K, Schild SE, et al. Radiation Therapy Oncology Group: A randomized phase III comparison of standard-dose (60 Gy) versus high-dose (74 Gy) conformal chemoradiotherapy with or without cetuximab for stage III non-small cell lung cancer: Results on radiation dose in RTOG 0617. *ASCO Meet Abstr* 2013;31:7501.
- [5] Hanna N, Neubauer M, Yiannoutsos C, McGarry R, Arseneau J, Ansari R, et al. Phase III Study of cisplatin, etoposide, and concurrent chest radiation with or without consolidation docetaxel in patients with inoperable stage III non-small-cell lung cancer: the Hoosier Oncology Group and U.S. Oncology. *J Clin Oncol* 2008;26:5755–60.
- [6] Kelly K, Chansky K, Gaspar LE, Albain KS, Jett J, Ung YC, et al. Phase III trial of maintenance gefitinib or placebo after concurrent chemoradiotherapy and docetaxel consolidation in inoperable stage III non-small-cell lung cancer: SWOG S0023. *J Clin Oncol Off J Am Soc Clin Oncol* 2008;26:2450–6.
- [7] Lambin P, Rios-Velazquez E, Leijenaar R, Carvalho S, Van Stiphout RGPM, Granton P, et al. Radiomics: extracting more information from medical images using advanced feature analysis. *Eur J Cancer* 2012;48:441–6.
- [8] Kumar V, Gu Y, Basu S, Berglund A, Eschrich SA, Schabath MB, et al. Radiomics: the process and the challenges. *Magn Reson Imaging* 2012;30:1234–48.
- [9] Lambin P, Van Stiphout RGPM, Starmans MHW, Rios-Velazquez E, Nalbantov G, Aerts HJWL, et al. Predicting outcomes in radiation oncology—multifactorial decision support systems. *Nat Rev Clin Oncol* 2013;10:27–40.
- [10] Rios Velazquez E, Aerts HJWL, Gu Y, Goldgof DB, De Ruyscher D, Dekker A, et al. A semiautomatic CT-based ensemble segmentation of lung tumors: comparison with oncologists' delineations and with the surgical specimen. *Radiother Oncol* 2012;105:167–73.
- [11] Parmar C, Rios Velazquez E, Leijenaar R, Jermoumi M, Carvalho S, Mak RH, et al. Robust radiomics feature quantification using semiautomatic volumetric segmentation. *PLoS One* 2014;9:e102107.
- [12] Leijenaar RTH, Carvalho S, Velazquez ER, van Elmpst WJC, Parmar C, Hoekstra OS, et al. Stability of FDG-PET Radiomics features: An integrated analysis of test-retest and inter-observer variability. *Acta Oncol* 2013;52:1391–7.
- [13] Ganeshan B: Non_small cell lung cancer: histopathologic correlates for texture parameters at CT. *Radiology*.
- [14] Davnall F, Yip CSP, Ljungqvist G, Selmi M, Ng F, Sanghera B, et al. Assessment of tumor heterogeneity: an emerging imaging tool for clinical practice? *Insights Imaging*. 2012;3:573–89.
- [15] Ganeshan B, Panayiotou E, Burnand K, Dizdarevic S, Miles K. Tumour heterogeneity in non-small cell lung carcinoma assessed by CT texture analysis: a potential marker of survival. *Eur Radiol* 2012;22:796–802.
- [16] Ganeshan B, Abaleke S, Young RCD, Chatwin CR, Miles KA. Texture analysis of non-small cell lung cancer on unenhanced computed tomography: initial evidence for a relationship with tumour glucose metabolism and stage. *Cancer Imaging* 2010;10:137–43.
- [17] He X, Sahiner B, Gallas BD, Chen W, Petrick N. Computerized characterization of lung nodule subtlety using thoracic CT images. *Phys Med Biol* 2014;59:897–910.
- [18] Skogen K, Ganeshan B, Good C, Critchley G, Miles K. Measurements of heterogeneity in gliomas on computed tomography relationship to tumour grade. *J Neurooncol* 2013;111:213–9.
- [19] Ravanelli M, Farina D, Morassi M, Roca E, Cavalleri G, Tassi G, et al. Texture analysis of advanced non-small cell lung cancer (NSCLC) on contrast-enhanced computed tomography: prediction of the response to the first-line chemotherapy. *Eur Radiol* 2013;23:3450–5.
- [20] Aerts HJWL, Velazquez ER, Leijenaar RTH, Parmar C, Grossmann P, Cavalho S. Decoding tumour phenotype by noninvasive imaging using a quantitative radiomics approach. *Nat Commun* 2014;5.
- [21] Chae H-D, Park CM, Park SJ, Lee SM, Kim KG, Goo JM. Computerized texture analysis of persistent part-solid ground-glass nodules: differentiation of preinvasive lesions from invasive pulmonary adenocarcinomas. *Radiology* 2014;132187.
- [22] Fried DV, Tucker SL, Zhou S, Liao Z, Mawlawi O. Prognostic value and reproducibility of pretreatment CT texture features in stage III non-small cell lung cancer. *Int J Radiat Oncol* 2014.
- [23] Vaidya M, Creach KM, Frye J, Dehdashti F, Bradley JD, El Naqa I. Combined PET/CT image characteristics for radiotherapy tumor response in lung cancer. *Radiother Oncol* 2012;102:239–45.
- [24] Aerts HJWL, Bussink J, Oyen WJG, van Elmpst W, Folgering AM, Emans D, et al. Identification of residual metabolic-active areas within NSCLC tumours using a pre-radiotherapy FDG-PET-CT scan: A prospective validation. *Lung Cancer* 2012;75:73–6.
- [25] Van Elmpst W, Das M, Hüllner M, Sharifi H, Zegers CML, Reymen B, et al. Characterization of tumor heterogeneity using dynamic contrast enhanced CT and FDG-PET in non-small cell lung cancer. *Radiother Oncol* 2013;109:65–70.
- [26] Balagurunathan Y, Gu Y, Wang H, Kumar V, Grove O, Hawkins S, et al. Reproducibility and prognosis of quantitative features extracted from CT images. *Transl Oncol* 2014;7:72–87.
- [27] Ball DL, Fisher RJ, Burmeister BH, Poulsen MG, Graham PH, Pennim MG, et al. The complex relationship between lung tumor volume and survival in patients with non-small cell lung cancer treated by definitive radiotherapy: a prospective, observational prognostic factor study of the Trans-Tasman Radiation Oncology Group (TROG 99.05). *Radiother Oncol* 2013;106:305–11.
- [28] Etiz D, Marks LB, Zhou S-M, Bentel GC, Clough R, Hernando ML. Influence of tumor volume on survival in patients irradiated for non-small-cell lung cancer. *Int J Radiat Oncol Biol Phys* 2002;53:835–46.
- [29] Alexander BM, Othus M, Caglar HB, Allen AM. Tumor volume is a prognostic factor in non-small-cell lung cancer treated with chemoradiotherapy. *Int J Radiat Oncol Biol Phys* 2011;1381–7.
- [30] Mirsadraee S. The 7th lung cancer TNM classification and staging system: review of the changes and implications. *World J Radiol* 2012;4.
- [31] Oken MM, Creech RH, Tormey DC, Horton J, Davis TE, McFadden ET, et al. Toxicity and response criteria of the Eastern Cooperative Oncology Group. *Am J Clin Oncol* 1982;5:649–55.
- [32] Deasy JO, Blanco AI, Clark VH. CERR: a computational environment for radiotherapy research. *Med Phys* 2003;30:979–85.
- [33] De Jay N, Papillon-Cavanagh S, Olsen C, El-Hachem N, Bontempi G, Haibe-Kains B. MRMRE: an R package for parallelized mRMR ensemble feature selection. *Bioinformatics* 2013;29:2365–8.
- [34] Schröder MS, Culhane AC, Quackenbush J, Haibe-Kains B. Survcomp: an R/Bioconductor package for performance assessment and comparison of survival models. *Bioinformatics* 2011;27:3206–8.
- [35] Lumley T: *Rmeta*. 2012.
- [36] Gentleman RC, Carey VJ, Bates DM, Bolstad B, Dettling M, Dudoit S, et al. Bioconductor: open software development for computational biology and bioinformatics. *Genome Biol* 2004;5:R80.
- [37] Harrell FE, Califf RM, Pryor DB, Lee KL, Rosati RA. Evaluating the yield of medical tests. *JAMA J Am Med Assoc* 1982;247:2543–6.
- [38] Benjamini Y, Hochberg Y. Controlling the false discovery rate: a practical and powerful approach to multiple testing. *J R Stat Soc Ser B Methodol* 1995;57:289–300.
- [39] Core Team R. R: a language and environment for statistical computing. Vienna, Austria: R Foundation for Statistical Computing; 2013, ISBN 3-900051-07-0. <http://www.R-Project.org/>.